Vogelstein, B., Pardoll, D. M., & Coffey, D. S. (1980) *Cell (Cambridge, Mass.) 22*, 79–85.
Wanka, F., Mullenders, L. H. F., Bekers, A. G. M., Pennings, L. J., Aelen, J. M. A., & Eygensteyn, J. (1977) *Biochem. Biophys. Res. Commun. 74*, 739–747.
Wunderlich, F. (1978) *Naturwiss. Rundsch. 31*, 282–288.
Wunderlich, F., & Herlan, G. (1977) *J. Cell Biol. 73*, 271–278.

Left Handed Double Helices: Effect of Sequence on the Spatial Configuration of High Anti Nucleic Acids†

M. M. Dhingra, Ramaswamy H. Sarma,* S. Uesugi, T. Shida, and M. Ikehara

ABSTRACT: The conformational properties of purine–pyrimidine and pyrimidine–purine dinucleoside monophosphates in which the glycosidic torsion is fixed to $\simeq 120°$ by the formation of a covalent link between the base and the sugar ring are explored by ^1H NMR spectroscopy in order to obtain information about the spatial configuration of high anti nucleic acids. The intramolecular stack of the high anti dimers were found to be left handed, in contrast to that (right handed) for natural oligomers, which are low anti. Even though both the high anti pyrimidine–purine and purine–pyrimidine dimers have similar backbone torsion angles, they display widely different relative geometry between the bases; thus in the former there is extensive base–base overlap in the stack, and in the latter there is negligible intramolecular base–base overlap. In addition it was found that purine–pyrimidine systems form miniature double helices in which there is substantial interstrand purine–purine interaction; on the other hand the pyridine–purine high anti dinucleosides have no proclivity to form such base-paired complexes in solution. Mathematical polymerization of the conformation of the high anti purine–pyrimidine dinucleoside monophosphates generates a left handed helix for high anti polynucleotides. This also means that the double helix for high anti nucleic acids containing purine–pyrimidine repeated units may also be left handed, as had been suggested [Sundaralingam, M., & Yathindra, N. (1977) *Int. J. Quantum Chem., Quantum Biol. Symp. 4*, 285]. It is suggested that the plasticity in the structure of genomic DNA is such that, if under certain conditions of interactions the sugar–base torsion of certain domains assume high anti values, that domain will become left handed, and this in turn can be a mechanism for the control of expression by genomic DNA.

It is well recognized that the variety in nucleic acid structures is accomplished primarily by the variations in the phosphodiester torsion angles and to a lesser extent by changes in other torsion angles (Sundaralingam, 1973, 1975; Sundaralingam & Westhof, 1979). Out of a total of nine staggered conformations possible by rotation about the phosphodieser bonds, only one conformation, having gauche–gauche (g^-g^-, $\omega' \simeq 290°$, $\omega \simeq 290°$; see Figure 1 for nomenclature) orientation, leads to a right handed helical organization (Yathindra & Sundaralingam, 1974; Pullman & Saran, 1976; Govil & Saran, 1971; Kim et al., 1973). The preferred ranges of the remaining torsion angles are $\phi \simeq 180°$, $\psi \simeq 60°$; the sugar could be either ^2E or ^3E; and the glycosidic torsion angle (χ) is in the anti range. Furthermore, the right handed helical organization is maintained even if the glycosidic torsion is toggled to syn orientation by introducing bulky substituents on C-8 of purines (Govil et al., 1977). However, recent single-crystal studies of self-complementary d-CGCGCG (Wang et al., 1979) and d-CGCG (Drew et al., 1980), fiber diffraction studies of poly(dG-dC)·poly(dG-dC) (Arnott et al., 1980), and NMR studies of poly(dG-dC)·(poly(dG-dC) (Mitra et al., 1981) have clearly shown that the various torsion angles can assume values so that a left handed double helix can be generated. Extensive theoretical investigations in several laboratories (Yathindra & Sundaralingam, 1976; Sundaralingam & Yathindra, 1977; Fujii & Tomita, 1976; Olson & Dasika, 1976; Olson, 1977) showed that the sense of base stack in high anti systems is left handed, but these calculations reach different conclusions with respect to the helical organization of the backbone.

The unusual CD spectra observed for model dimers (Ikehara et al., 1970; 1974) A^spA^s and A^opA^o (in which the glycosidic torsion is fixed in high anti orientation, $\simeq 120°$, by covalent linkage between the sugar and the base moieties; see Figure 1 and legend for abbreviations) are approximate mirror images of the unmodified ApA in which the glycosidic torsion is in the anti domain. The inverted CD spectra of these high anti systems indicate that the sense of base stack is left handed in contrast to the right handed stacking observed for ApA. This means that the ratio of the base stacking parameters (Olson, 1976) Z/θ (Z = vertical displacement of the stacked bases, θ = the base stacking angle) is positive for ApA and negative for cyclodimers A^spA^s and A^opA^o. The complete chemical shift and (Dhingra et al., 1978) proton dimerization shifts observed for A^spA^s in aqueous solution indicate that A^spA^s adopts a left handed base-stacked geometry. The backbone torsion angles and base-stacking parameters determined by Dhingra et al. (1978) for A^spA^s are in agreement with those predicted by theoretical calculations (Fujii & Tomita, 1976).

Olson & Dasika (1976) have claimed that the left handed stacking does not necessarily mean that the helical sense is left handed. From their geometrical calculations, they found that single- and double-stranded polycyclonucleotides with glycosidic torsion in the high anti ($\chi_{CN} \approx 120°$) prefer a left handed base stacking with a right handed helical organization

† From the Institute of Biomolecular Stereodynamics, State University of New York at Albany, Albany, New York 12222, and the Faculty of Pharmaceutical Sciences, Osaka University, 133-1 Yamadakami Suita, Osaka, Japan. *Received January 5, 1981.* This work was supported by Grant CA12462 from the National Cancer Institute, Department of Health, Education and Welfare, and Grant PCM7822531 from the National Science Foundation.

0006-2960/81/0420-5002$01.25/0

Table I: Proton Chemical Shifts[a] for Cyclonucleotides

nucleotide	temp (°C)	1′	2′	3′	4′	5′	5″	2	5
pU^o	22	3.300	2.273	1.482	1.264	0.647	0.624		2.092
	85	3.302	2.275	1.474	1.249	0.660	0.654		2.118
U^op	22	3.347	2.431	1.659	1.311	0.484	0.437		2.074
	85	3.326	2.453	1.670	1.300	0.496	0.418		2.105
A^sp	20	3.431	1.904	1.680	1.211	0.565	0.439	4.852	
	70	3.511	2.028	1.710	1.249	0.558	0.429	4.989	
pA^s	20	3.452	1.839	1.528	1.233	0.707	0.633	4.892	
	70	3.493	1.839	1.528	1.232	0.724	0.650	4.963	
A^spU^o	22 A^sp	3.320	1.840	1.625	1.107	0.591	0.437	4.605	
	pU^o	3.260	2.335	1.491	1.220	0.915	0.773		2.101
	85 A^sp	3.474	1.954	1.655	1.184	0.520	0.395	4.988	
	pU^o	3.291	2.291	1.488	1.250	0.795	0.744		2.107
U^opA^s	22 U^op	2.948	2.130	1.418	1.045	0.305	0.229		1.848
	pA^s	3.360	1.842	1.528	1.152	0.943	0.795	4.830	
	85 U^op	3.075	2.179	1.477	1.082	0.332	0.242		1.965
	pA^s	3.456	1.840	1.518	1.200	0.895	0.778	4.995	

[a] In parts per million from internal tetramethylammonium chloride.

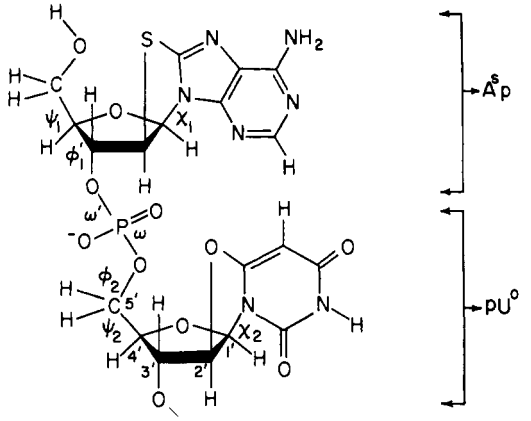

FIGURE 1: Nomenclature and the basic structure of A^spU^o. The designation A^s means adenine C-8 linked to sugar C-2′ by sulfur; U^o means uracil C-6 linked to sugar C-2′ by oxygen; etc.

for the backbone (Olson & Dasika, 1976; Olson, 1977). Such an unusual character of the model requires base planes to be parallel to the helix axis. On the other hand, Fujii & Tomita (1976) found that a left handed stack of A^spA^s with phosphodiester torsions in the g^-g^- domain is energetically favored and a regular left handed helical structure with a left handed stack is a stable conformation for poly(A^s). They also showed that a set of smaller ω' and ω values, relative to those for a right handed helix, in the g^-g^- domain can generate a left handed helix. From helical parameter analysis, Sundaralingam & Yathindra (1977) obtained the same conclusion and proposed a similar model, a left handed helix with a left handed stack, for polyribonucleotides with high anti glycosidic conformation. In their models, the base planes are perpendicular to the helix axis, like Arnott & Hukins's (1972) B-DNA, but the helical organization is left handed.

Recently Mitra et al. (1980) examined the base stacking patterns in the Olson right handed and Sundaralingam left handed models vis-â-vis the pattern in the miniature double helix.

They concluded that the significant interstrand base stacking and little intrastrand base stacking noted in the above minihelix agrees with the right handed Olson model and disagrees with the *specific* left handed model of Sundaralingam. At the same time Mitra et al. (1980) stressed "we have not made a search to determine whether left handed helices with significant interstrand and little intrastrand base stacking are possible for high anti polynucleotides".

In this paper we attempt to determine the helical sense of the backbone of high anti nucleic acids by extensive ^{1}HNMR studies of the sequence isomers A^spU^o and U^opA^s (Figure 1) and the corresponding mononucleotides A^sp, pA^s, U^op, and pU^o, in all of which glycosidic torsion is chemically fixed at $\simeq 120°$.

Experimental Procedures

The sequence isomers of dinucleoside monophosphates (8,2′-andhyro-8-thio-9-β-D-arabinofuranosyladeninyl-3′-phosphoryl-(3′–5′)-6,2′-anhydro-6-oxy-1-β-D-arabinofuranosyluracil (A^spU^o), and 6,2′-anhdyro-6-oxy-1-β-D-arabinofuranosyluracilyl-3′-phosphoryl-(3′–5′)-8,2′-anhydro-8-thio-9-β-D-arabinofuranosyladenein (U^opA^s) and the monomers A^sp, pA^s, U^op, and pU^o were synthesized by condensation of properly protected nucleoside and nucleotide units using DCC as condensing agent. The details of the synthesis are presented elsewhere (Ikehara et al., 1980). All the samples were lyophilysed 3 times from 99.8% D_2O and the final solutions were made in 100% D_2O. The pD (pH +0.4) was measured with a Fisher Accument Model 320 pH meter and were 7.5 and 5.5 for the dimer and monomers, respectively.

Proton magnetic resonance spectra were recorded on a Bruker 270-MHz spectreomter located at Yale University (Southern New England High Field Facility). Tetramethylammonium chloride (TMA) was used as internal calibrant. The spectra for complete analysis were recorded as a function of temperature (15–85 °C) and concentration (2.5–80 mM). The spectra for investigating self-associative properties were recorded in 4 M LiCl solutions in the temperature range −15 to 45 °C.

The spectra were analyzed by using LAOCN III and the NMR parameters are accurate to ±0.005 ppm for chemical shifts and ±0.1-Hz coupling constants. The error in coupling constants for LiCl solutions at low temperatures is ±0.4 Hz. The observed and simulated spectra for the dimers and the monomers are shown in Figures 2–4. The chemical shifts and coupling constants are summarized in Tables I and II. Absolute assignments of CH-5′ and CH-5″ of the backbone are not possible now. We have assumed the empirical Remin & Shugar (1972) assignments in which the low-field lines in the ABX-type spectrum arise from H-5′ and the high-field lines from H-5″.

Table II: Coupling Constants[a] in Cyclonucleotides

nucleotide	temp (°C)	1',2'	2',3'	3',4'	4',5'	4',5''	5',5''	3',P	4',P	5',P	5'',P	2',4'
pU^o	22	5.4	0.6	2.2	4.7	5.9	−11.9		0.7	5.2	6.5	0.5
	85	5.5	0.8	2.5	5.7	5.7	−11.8		0.7	6.2	6.2	0.7
U^op	22	5.4	0.4	1.8	4.1	4.7	−13.0	8.3				0.5
	85	5.4	0.8	1.8	4.2	5.9	−12.8	8.3				0.4
A^sp	22	6.8	2.8	4.1	3.7	6.1	−12.9	7.5				
	70	6.8	2.5	3.5	4.6	6.2	−12.6	7.3				
pA^s	22	6.7	2.7	3.3	5.3	6.1	−11.5			5.8	6.9	
	70	6.7	2.7	3.2	5.3	6.2	−11.6			5.8	6.5	
U^opA^s	22 U^op	5.8	1.0	2.8	3.7	4.6	−12.9	8.0				0.8
	pA^s	6.8	3.5	5.6	3.1	4.3	−11.7		1.5	4.9	4.9	0.8
	85 U^op	5.5	0.9	2.8	4.1	5.6	−12.6	8.1				0.9
	pA	6.8	3.2	4.3	3.9	5.6	−11.8		1.1	5.4	5.7	0.8
A^apU^o	22 A^sp	6.7	3.4	5.1	3.2	5.2	−12.8	7.2				0.6
	pU^o	5.5	1.9	4.5	2.9	4.8	−11.8		1.5	4.8	5.6	0.3
	85 A^sp	6.8	2.7	3.8	4.4	6.3	−12.4	7.2				0.8
	pU	5.6	0.9	3.3	4.3	5.6	−12.0		0.6	5.8	6.1	0.5

[a] In hertz.

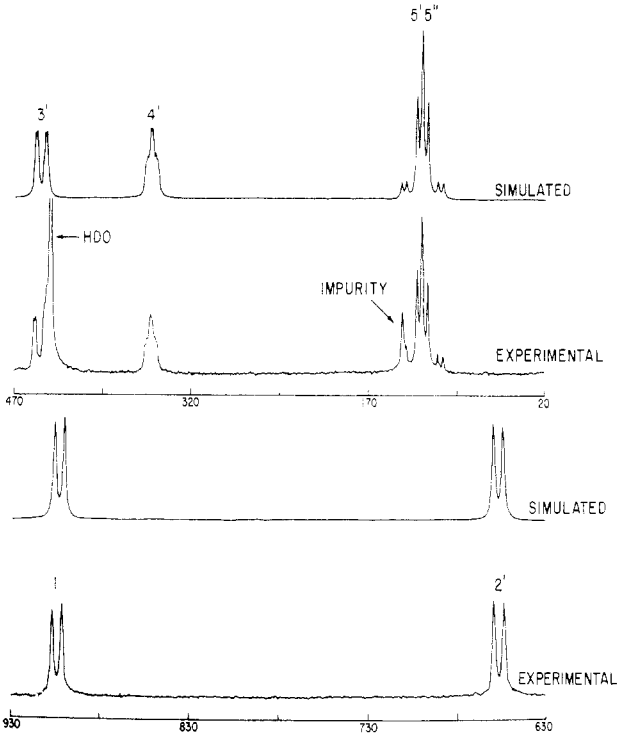

FIGURE 2: Experimental and computer-simulated 270-MHz ^1H NMR spectrum of U^op at 22 °C; shifts are in hertz with respect to internal tetramethylammonium chloride.

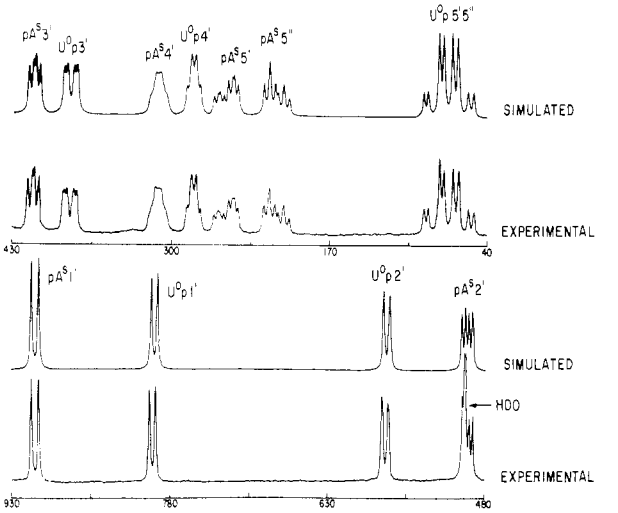

FIGURE 3: Experimental and computer-simulated 270-MHz ^1H NMR spectrum of U^opA^s, 22 °C.

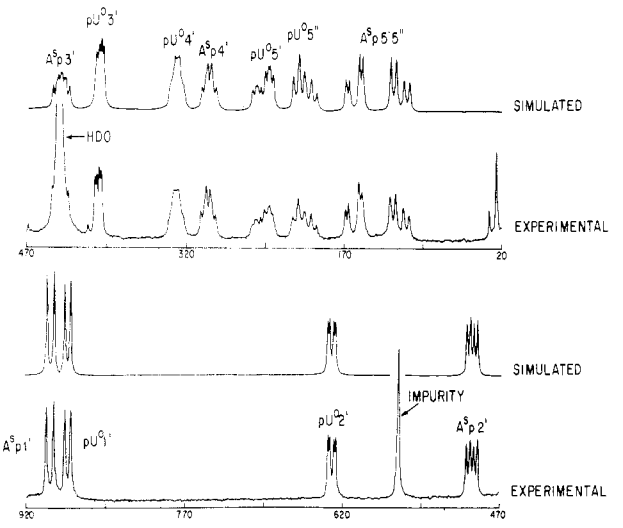

FIGURE 4: Experimental and computer-simulated 270-MHz ^1H NMR spectrum of A^spU^o, 22 °C.

In this paper we employ the Karplus equation to derive the population of conformers about the various bonds. We arrive at the geometry of the molecules by computing magnetic shelding constants from *xyz* coordinates taking into consideration the contribution to shielding from ring current fields and from the paramagnetic and diamagnetic components of atomic magnetic anisotropy. We have documented in detail elsewhere (Evans & Sarma, 1974, 1975; Lee & Sarma, 1975, 1976; Lee et al., 1975) the error limitations in the Karplus approach; even though there may be errors up to 10% in the absolute values of the populations, the data are very reliable for *comparing* conformational preferences among a series of analogous compounds. Recently we have described in detail (Mitra et al., 1981) the errors and limitations involved in the derivation of magnetic shielding constants and their application to obtain molecular conformation. Even though the application of the Karplus relations and magnetic shielding constants generate hard data, this should not be interpreted to mean that the treatment results in a precise knowledge of the exact geometry and the exact percentage; rather it indicates definitive trends. For example, if the percentage *gg* about C-4'–C-5' changes from 32 in the monomer to 62 in the dimer, the change of 30% is real, but the absolute values of 32 and 62 could be off by as much as 10% in the *same direction*.

Table III: Population Distribution of Conformers in Cyclonucleotides

		dimer				monomer			
		arabinose ring	backbone			arabinose ring	backbone		
nucleotide	temp (°C)	$J_{1',2'} + J_{3',4'}$ (Hz)	% *gg*	% *g'g'*	θ_{PH} (deg)	$J_{1',2'} + J_{3',4'}$ (Hz)	% *gg*	% *g'g'*	θ_{PH} (deg)
pU^o	22					7.6	32	64	
	85					8.0	24	61	
U^op	22					7.2	50		±33
	85					7.2	37		±33
pA^s	22					10.0	24	60	
	70					9.9	23	61	
A^sp	22					10.9	40		±39
	70					10.3	30		±40
A^spU^o	22 A^sp	11.8	55		±39				
	pU^o	10.0	62	70					
	85 A^sp	10.6	31		±39				
	pU^o	8.9	39	63					
U^opA^s	22 U^op	8.6	55		±35				
	pA^s	12.4	65	73					
	85 U^op	8.3	41		±34				
	pA^s	11.1	43	67					

It should further be noted that we employ conformational designations such as *gg*, *g'g'*, ^2E, ^3E, etc., to indicate domains rather than precise geometry, i.e., ^3E pucker should not be taken to mean a conformation in which the phase angle of pseudorotation is precisely 18°, but conformations centered around the domain of 18°. In great detail Evans & Sarma (1974) have discussed that the Karplus approach cannot be used to pinpoint the precise sugar pucker and the best way to treat all five-membered sugars is to assume $^2E \rightleftharpoons {}^3E$ equilibria.

Results and Discussion

Conformation of the Sugar Ring. The sugar ring in A^spU^o and U^opA^s is an arabinose. The detailed treatment of the arabinose ring conformation is presented elsewhere (Dhingra et al., 1978a,b), and it was shown to display the conventional C(2')-endo (^2E) $\rightleftharpoons$ C(3')-endo (^3E) equilibrium. It will suffice to say here that the constancy of the sum $J_{1',2'} + J_{3',4'}$ cannot be used to estimate the equilibrium populations of ^2E and ^3E conformers as is the case for the ribose ring (Lee et al., 1976; Ezra et al., 1977). This is because in the arabinose case this sum is variable. In the arabinose system for ^2E puckers both $J_{1',2'}$ and $J_{3',4'}$ are gauche couplings; for ^3E pucker one is gauche and the other trans coupling, so much so that the sum $J_{1',2'} + J_{3',4'}$ is going to be larger for ^3E pucker than for ^2E. Therefore the displacement of equilibrium will not entail the constancy of this sum. However, an increment in the sum will be indicative of the increased population of ^3E pucker. Examination of the data in Table III reveals that in going from monomers to the dimers, the sum $J_{1',2'} + J_{3',4'}$ for the 5'-nucleotidyl unit irrespective of whether the base is purine or pyrimidine registers an increase of about 2.4 Hz while the sum for the 3'-nucleotidyl unit increases by about 1.0 Hz. A comparison of the magnitudes of $J_{3',4'}$ and $J_{1',2'}$ (Table II) for the 5'-nucleotidyl unit for the dimer with the corresponding monomer suggests that the gain in the sum $J_{1',2'} + J_{3',4'}$ is predominantly due to an increase in the magnitude of $J_{3',4'}$. This increase in the magnitude of $J_{3',4'}$ definitely indicates an increase in the population of ^3E conformers. A similar argument for 3'-nucleotidyl unit is also valid, but the increase in the magnitude of $J_{3',4'}$ is relatively smaller. Hence one may conclude that upon dimerization the equlibrium $^2E \rightleftarrows {}^3E$ is displaced more toward ^3E.

The near-constancy of the sum $J_{1',2'} + J_{3',4'}$ for the monomers with variation in temperature indicates insensitivity of equilibrium to temperature while in the dimers the sum $J_{1',2'} + J_{3',4'}$ decreases at high temperature. This decrease in the sum for the dimers suggests a greater degree of flexibility for the arabinose ring *in the dimers* even under the constraint of cyclization between the base and the sugar ring involving the 2'-carbon atom.

The long-range four-bond ^1H–^1H coupling constant $J_{2',4'}$ (Table III) has been estimated for cyclonucleotides from the line-shape analysis. No attempt has been made to make conformational deductions because the magnitude of the coupling constant is small (0.4–0.8 Hz), and this has been pointed out earlier by several investigators (Hall & Manville, 1968; Dhingra & Sarma, 1979). However, the observation of $J_{2',4'}$ supports the presence of ^2E conformers because in this sugar pucker the H-2' and H-4' protons are in an in-plane zig-zag "W" arrangement.

Conformation about the C-4'–C-5' and C-5'–O-5' Bonds. The conformational preferences about the C-4'–C-5' and C-5'–O-5' bonds manifest themselves in the sum of the coupling constants $J_{H\text{-}4'\text{-}H\text{-}5'} + J_{H\text{-}4'\text{-}H\text{-}5''}$ and $J_{H\text{-}5'\text{-}P} + J_{H\text{-}5''\text{-}P}$, respectively. The population of the conformers about these bonds [see Sarma (1980) for the Newman projections of these conformers] was calculated by using the expressions reported by Lee & Sarma (1976).

The estimated populations for the gauche–gauche (*gg*, ψ = 60°) orientation about the C-4'–C-5' bond are given in Table III. Examination of the data in Table III reveals that the monomers have clear bias for the *gt*/*tg* orientation about the C-4'–C-5' bond irrespective of the base and the phosphate position. A comparison of 5'- and 3'-nucleotides indicates that 5'-monophosphates irrespective of the base have a smaller percentage of *gg* conformer than the 3'-monophosphates. Within the 5'-mononucleotides/3'-nucleotides, uridine mononucleotides have relatively greater population of *gg* conformer. The elevation of temperature further decreases the population of *gg* conformers in all the monomers, but the effect is relatively more pronounced (10–13%) in 3'-mononucleotides. On the other hand, the population of *g'g'* about the C-5'–O-5' bond is around 60% and exhibits a bias for *g'g'* orientation. It is concluded that monomers have a bias for the *gt*/*tg* orientation about the C-4'–C-5' bond while the preferred conformation about C-5'–O-5' bond is *g'g'*. Hence the preferred conformation for the cyclomononucleotides A^sp, pA^s, U^op, and pU^o is high anti ($^2E \rightleftarrows {}^3E$) *g*/*t*–*g'g'* which is very similar to that observed in the 8-aza analogues of 5'AMP and 5'GMP (Lee et al., 1975). The occurrence of the *g*/*t*–*g'g'* confor-

Table IV: Dimerization Shifts

nucleotide	temp (°C)	unit	$\delta_{monomer} - \delta_{dimer}$ 1′	2′	3′	4′	5′	5″	2	5
$U^{o}pA^{s}$	22	$U^{o}p$	0.399	0.301	0.241	0.266	0.179	0.208		0.226
		$-pA^{s}$	0.092	0.000	0.000	0.081	−0.237	−0.162	0.059	
	85	$U^{o}p-$	0.250	0.274	0.194	0.218	0.163	0.175		0.140
		$-pA^{s}$	0.037	−0.001	0.010	0.031	−0.171	−0.128	−0.032	
$A^{s}pU^{o}$	22	$A^{s}p-$	0.111	0.064	0.055	0.104	−0.026	0.000	0.247	
		$-pU^{o}$	0.040	−0.062	−0.009	0.045	−0.268	−0.148		−0.009
	85	$A^{s}p-$	0.037	0.074	0.055	0.065	0.038	0.034	0.001	
		$-pU^{o}$	0.011	−0.016	−0.014	−0.001	−0.135	−0.090		0.011

mational framework for both 3′- and 5′-cyclonucleotides is rather unexpected and suggests that not only is the repulsive interaction between the phosphate group and the lone-pair electrons on the sulfur/oxygen atom responsible for this conformation but also the interaction between the 5′-oxygen and the lone-pair electrons on sulfur/oxygen atoms at the site of cyclization.

The data for the dimers (Table III) indicate that dimerization brings about significant increase in the population of *gg* conformers (up to 40%) while the *g′g′* population increases to the extent of 13%. The 5′-nucleotidyl unit of the dimers, irrespective of the nature of the base, registers an increase of 30–40% in the population *gg* conformer while the 3′ unit gains about 5–15%. This switching over of the preference from *gt*/*tg* orientation in the monomers to *gg* conformation in the dimer must be accompanied by some adjustments in other torsion angles.

The increase of temperatures seems to have a much larger effect on the dimers than on the monomers, and the population of *gg* conformer decreases by about 24% for both the units of $A^{s}pU^{o}$ and 14–22% for $U^{o}pA^{s}$. In $A^{s}pU^{o}$ dimer the *gg* population for both the nucleotidyl units is reduced close to the monomer values at 85 °C. The conformational preference about C-5′–O-5′ is relatively less sensitive to temperature, and the population of the *g′g′* conformer decreases by about 7% in both the dimers.

Conformation about the C-3′–O-3′ Bond (ϕ'). In principle there are three staggered rotamers possible about C-3′–O-3′ bonds: these are the P–O-3′ bond trans to C-3′–C-4′ (ϕ' = 180°, α^{-} domain), the P–O-3′ bond trans to C-3′–C-2′ (ϕ' = 300°, α^{+} domain), and the P–O-3′ bond gauche to both C-3′–C-4′ and C-3′–C-2′ (ϕ' = 60°, trans). The conformational preference about this bond manifests itself in the vicinal coupling constant $J_{H\text{-}3'\text{-}P}$. The magnitude of the observed coupling ranges from 8.0 to 8.3 Hz (Table II) for the $U^{o}p$-unit while for the $A^{s}p$ unit the value of this coupling constant lies in the range 7.2–7.5 Hz. The dihedral angle H–C-3′–O-3′–P can be computed for these observed coupling constants by using the Karplus equation, i.e., $^{3}J_{HP} = 18.1 \cos^{2}\theta_{PH} - 4.8 \cos\theta_{PH}$. The calculated dihedral angles θ_{PH} ±33–35° (for the $U^{o}p$ unit) and ±39–40° (for the $A^{s}p$ unit), which are in the allowed ranges on the basis of steric considerations, are given in Table III. These values could be either in α^{-} (ϕ' = 207–200°) or in α^{+} (ϕ' = 273–280°) domains, ϕ being equal to 240° ± θ_{PH}. the presence of the trans conformation (ϕ' = 60°) is excluded because such a conformation is never encountered in crystal structures (Rosenberg et al., 1976; Seeman et al., 1976) and also is predicted to be of higher energy by theoretical calculations (Pullman et al., 1972; Govil, 1976). Evidence has been presented for the interrelationship (Sarma & Danyluk, 1977) between the sugar pucker and the torsion about the C-3′–O-3 bond. The α^{+} orientation of the 3′-phosphate favors ^{2}E while α^{-} orientation favors ^{3}E. The exclusion of trans conformer essentially leads to equilibrium between α^{+} and α^{-} conformers. Occasionally the availability of additional coupling $^{4}J_{2',P}$ helps in determining the preference for a particular conformer. There is no direct method of finding the preference for a particular conformer about the C-3′–O-3′ bond. However it is reasonable to conclude from the conformational nexus between the sugar pucker and ϕ' (Sarma, 1980a,b) that in dimers for those fractional populations in which sugar pucker is ^{3}E, $\phi \simeq 200°$, and for those in which sugar pucker is ^{2}E, $\phi' \simeq 280°$. The dimerization and temperature do not bring about any significant change in the magnitude of $J_{H\text{-}3'\text{-}P}$. The monomers seem to preserve the torsional preference about C-3′–O-3′ when they get incorporated into dimers.

Glycosidic Torsion Angle. In the cyclonucleotides examined here the conformational freedom about the sugar–base glycosyl bond is restricted because the C-8 of adenine or the C-6 or uracil is chemically linked to the arabinose 2′ carbon, and the magnitude of χ_{CN} is expected to be around 100–130°. In fact a value of 122° has been reported for 8,2′-cycloadenosine 3′,5′-phosphate (Tomita et al., 1972) and 114° for 6,2′-anhydro-1-β-D-arabinofuranosylcytosine (Kashitani et al., 1976) from single-crystal X-ray studies. The changes in the sugar and C-4′–C-5′ conformation upon dimerization discussed above lead us to suggest that incorporation of the cyclomononucleotide into the corresponding dinucleoside monophosphate causes some readjustment in χ.

Dimerization Shifts. The dimerization shift is the shift difference between a proton of the monomer and the corresponding proton in the dimer at the same temperature and other experimental conditions. The dimerization shifts result as a consequence of base stacking interactions, the magnitude and sign of the shift depends upon the geometry of the base stack.

The proton dimerization shift data for $A^{s}pU^{o}$ and $U^{o}pA^{s}$ at 22 and 85 °C are given in Table IV. A comparison of the dimerization shift data at 22 °C (Table IV) for the protons of $U^{o}p-$ and $-pU^{o}$ segments in the sequence isomers $U^{o}pA^{s}$ and $A^{s}pU^{o}$ indicates that the magnitude of shifts for all the protons are very much larger in $U^{o}pA^{s}$ than the shifts of the corresponding protons in $A^{s}pU^{o}$. Though the effect of sequence is noticeable in nucleic acid dimers (Lee et al., 1976; Ezra et al., 1977; Cheng & Sarma, 1977), the very small dimerization shifts for the $-pU^{o}$ segment in $A^{s}pU^{o}$ indicates that there is very little interaction between adenine and uridine bases. Normally one would have expected a similar pattern of dimerization shifts for uridine base and sugar protons in $A^{s}pU^{o}$ and in $U^{o}pA^{s}$, as is usually observed in nucleic acid dimers (Lee et al., 1976; Ezra et al., 1977; Cheng & Sarma, 1977). A glaring difference is the small downfield shift on δ H-5 of $-pU^{o}$ moiety of $A^{s}pU^{o}$ upon dimerization. In contrast, in ApU, the H-5 of -pU is shifted upfield by about 0.2 ppm upon dimerization. The negligible shift of H-5 of $-pU^{o}$ suggests practically no overlap between adenine and uracil bases. This is also evident from the shift pattern of the sugar protons of $-pU^{o}$

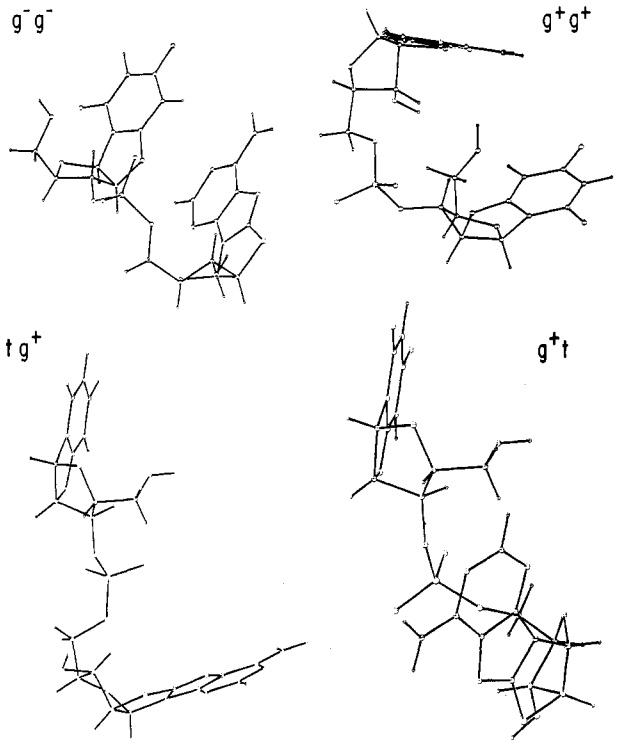

FIGURE 5: The four different geometries of U°pA^s in which the phosphodiester torsion assumes the g^-g^-, g^+g^+, tg^+, and g^+t conformations. See Tables V and VI.

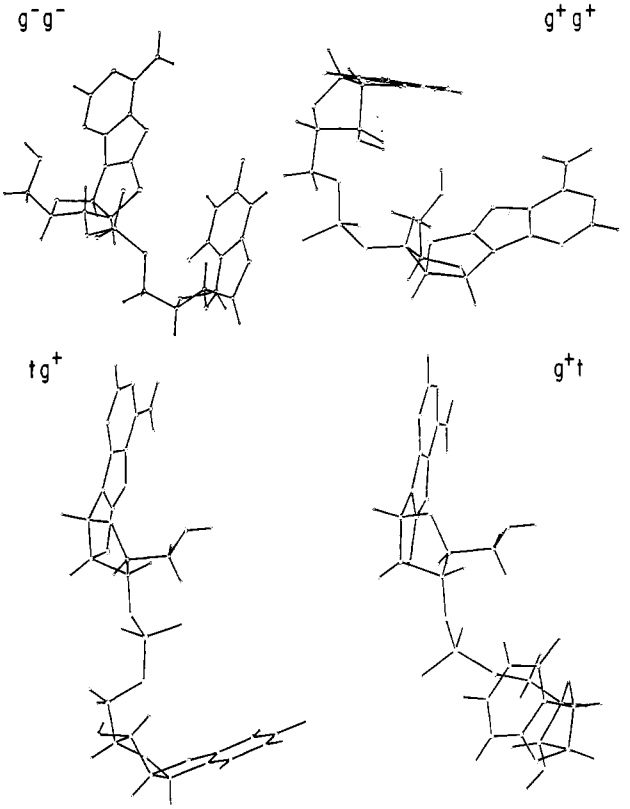

FIGURE 6: The four different geometries of A^{s}pU° in which the phosphodiester torsion assumes the g^-g^-, g^+g^+, tg^+, and g^+t conformations. See Tables VII and VII.

moiety of A^{s}pU° which do not seem to be influenced by the ring current field and magnetic anisotropy effects of adenine and is in contrast to what is observed in ApU. The significant upfield shift of H-2 of A^{s}p- of A^{s}pU° (Table IV) is bizarre because it cannot originate from intramolecularly stacked arrays for two reasons: (a) as detailed above in A^{s}pU°, there is little intramolecular base–base overlap, and (b) even if such overlaps were present, one does not expect the uridine to shield the adenine H-2 because the shielding from the ring current and magnetic anisotropy effects of uracil are small.

On the other hand in U°pA^s, the significant upfield shifts for the H-5 proton and all the sugar protons (Table IV) of the U°p segment indicate substantial base–base interaction and overlap. This kind of shift pattern is in line wiit those normally observed for nucleic acid dimers like UpA, CpG, CpA, etc. (Ezra et al., 1977) and arise from the shielding effect of purine base at the 3′ end. Much smaller shifts for the protons of -pA^s segment in U°pA^s are also expected and is observed (Table IV) because the uracil ring has relatively smaller shielding effects. The dimerization shift data for U°pA^s clearly suggest an intramolecular base-stacked geometry while the dimerization shift data for A^{s}pU° indicate no base–base interaction and overlap. *The data thus clearly indicate the profound effect of sequence on spatial configurations in nucleic acid structures.*

The Conformational Blend. We have provided documented evidence that nucleic acid structures at the oligonucleotide level in aqueous solution are conformationally pluralistic and in most cases exist as a conformational blend (Sarma, 1980b; Dhingra et al., 1978a,b) in which the phosphodiester torsion assumes the geometries of g^-g^-, g^+t, g^+g^+, and tg^+ (Figures 5 and 6). We have presented elsewhere (Dhingra et al., 1978a,b) the methods to determine this conformational blend. Essentially, the cartesian coordinates x, y, z for the various possible conformers are first converted into cylindrical coordinates and then total shielding/deshielding is estimated by summing up the contribution from ring-current effects and from the diamagnetic and paramagnetic components of the atomic magnetic anisotropy. The method is based on a iterative procedure where the torsion angles ω' and ω are varied in steps of 5° in

Table V: Projected Shielding for the Protons of U°p- of U°pA^s in Various Conformers

proton	conformer[a] g^-g^-	g^+t	g^+g^+	tg^+	scaled[b] δ_{total}	δ_{obsd}
H-1′	0.11	0.13	0.07	0.05	0.11	0.399
H-2′	0.37	0.25	0.14	0.07	0.28	0.301
H-3′	0.40	0.22	0.29	0.18	0.30	0.241
H-4′	0.05	0.51	0.07	0.08	0.28	0.265
H-5′	0.05	0.07	0.02	0.08	0.05	0.179
H-5″	0.13	0.24	0.06	0.17	0.17	0.208
H-5	0.37	0.06	0.21	0.08	0.20	0.226

[a] g^-g^- (ω' = 255°, ω = 270°), g^+t (ω' = 125°, ω = 225°), g^+g^+ (ω' = 80°, ω = 80°), tg^+ (ω' = 180°, ω = 80°); sugar = ^3E; the rest of torsion angles are the preferred ones (Table III). [b] 50% g^+t + 40% g^-g^- + 10% g^+g^+.

Table VI: Projected Shielding[a] for the Protons of the -pA^s Unit of U°pA^s in Various Conformers

proton	conformer[b] g^-g^-	g^+t	g^+g^+	tg^+	scaled[c] δ	δ_{obsd}
H-1′	−0.02	0.01	0.02	−0.01	0.00	0.09
H-2′	−0.02	0.00	0.02	−0.01	0.00	0.00
H-3′	−0.04	−0.01	0.07	−0.01	0.00	0.00
H-4′	−0.02	0.00	0.01	−0.01	0.00	0.08
H-5′	−0.03	0.01	−0.01	−0.03	0.00	−0.24
H-5″	−0.02	−0.01	0.00	−0.02	0.00	−0.16
H-2	0.16	0.00	−0.02	0.00	0.06	0.06

[a] In parts per million. [b] g^-g^- (ω' = 255°, ω = 270°), g^+t (ω' = 125°, ω = 225°), g^+g^+ (ω' = 80°, ω = 80°), tg^+ (ω' = 180°, ω = 80°); sugar pucker ^3E; the rest of the torsion angles are the preferred ones (Table III). [c] 40% g^-g^-.

the preferred conformational domains until a good fit is obtained for protons which are expected to be affected by the bases. The projected shielding alonge with the observed shifts for both the segments of U°pA^s for the g^-g^-, g^+t, g^+g^+, and tg^+ (Figure 5) conformers are given in Tables V and VI.

The examination of Tables V and VI shows that in the g^-g^- conformation the projected shielding for H-5, H-2′, and H-3′ are quite significant and are relatively larger than the observed shift, while the projected shieldings for H-1′, H-4′, and H-5′ protons are much smaller than the observed shifts. This pattern of projected shielding for the g^-g^- conformer is inconsistent with the observed shift and argues against *exclusive* presence (100%) of g^-g^- conformers; further, the inconsistency cannot be removed by varying ω' and ω torsions in the g^-g^- domain.

In the g^+t conformer, the presence of which is suggested from the upfield shift of H-4, H-5′, and H-5″ of the U°p- unit, the shielding is largest for H-4′ and almost twice the observed shift. The projected shieldings for the base protons H-5, H-1′, and H-5′ are much smaller than the experimentally observed shifts. The assumption that U°pA^s exists *exclusively* in the g^+t conformation (100%) is inconsistent with the pattern of observed shifts. However, inspection of the data in Table V suggests that in order to rationalize the observed shift of H-4′, it is imperative that the U°pA^s dimer must have some population of g^+t conformer because in all other conformers the projected shieldings for H-4′ are much smaller than what is observed.

In g^+g^+ conformer, the projected shieldings for H-5 and H-3′ are very close to the observed shifts while the projected shifts of H-1′, H-4′, H-5′, and H-5″ are much smaller than the observed ones. Similarly in the tg^+ conformer, the projected shieldings for H-3′ and H-5″ are close to the experimental shifts while the shifts for H-1′, H-2′, H-4′, H-5′, and H-5″ are much smaller. The existence of U°pA^s exclusively in g^+g^+/tg^+ conformations or in combination cannot explain the observed shifts for all the protons of the U°p- segment of U°pA^s; i.e., no single conformation can account for the pattern of the observed shifts. Hence it is reasonable to conclude that U°pA^s must exist in solution as an equilibrium mixture of all four conformers. The rationalization of the shift of H-4′ of U°p- residue requires at least 50% of the g^+t conformer because in all other conformations the projected shieldings for this proton are much smaller than the observed shifts. A 50% population of g^+t, however, cannot explain the shift of the remaining protons. However a blend of three conformers, g^-g^-, g^+t, and g^+g^+, in the ratio 50:40:10 reasonably explains the observed shift for at least five out of a total of seven protons (shown in Table V). There is no way to either estimate the population of tg^+ or omit this conformer from thhe blend. The discrepancy for the H-1′ proton shift is probably due to the fluctuations in χ_{CN} which are indicated in the analysis of sugar conformation in conjunction with the effect of the oxygen atom of the additional five-membered ring. This discrepancy was also noticed for H-1′ of the A^{s}pA^s dimer (Dhingra et al., 1978a,b). The disagreement between the observed and projected shifts for H-5′ could be because of switchover in the orientation of C-4′–C-5′, and this might be affecting H-5′ relatively more than H-4′ and H-5″.

The dimerization shift data for the -pA^s segment of U°pA^s (Table VI) shows that only two protons, i.e., H-5′ and H-5″, have significant dimerization shifts, and these protons are shifted downfield relative to the monomer. These downfield shifts are not unique to this molecule but have been observed in practically all nucleic acid dimers which show populations

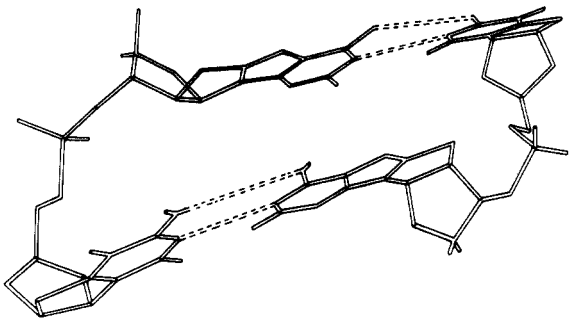

FIGURE 7: Structure of the self-complementary miniature double helix of A^{s}pU° [adapted from Sarma (1980c)].

of g^-g^- conformers (Lee et al., 1976; Ezra et al., 1977; Cheng & Sarma, 1977). The population distribution of the various conformers cannot be deduced from the dimerization data for the various protons in the -pA^s segment of U°pA^s because the calculated and the observed shifts are very small (Table VI). However the observed upfield shift of H-2 (0.06 ppm) can be rationalized only if it is assumed that 40% g^-g^- conformer is present. This conclusion for U°pA^s supports our earlier deductions from the dimerization shift data from the U°p segment. Hence it is concluded that U°pA^s exists in aqueous solution as an equilibrium blend of base-stacked (g^-g^-, g^+g^+), skewed (g^+t), and extended (tg^+) arrays (Figure 5).

The pattern of dimerization shifts observed (Table IV) for all the protons of both the segments of A^{s}pU° are bizarre except for the downfield shifts of H-5′ and H-5″ of the pU° segment. As has been noted before, these downfield shifts are indicative of the presence of g^-g^- conformers (Figure 6), the base-stacked geometry in normal nucleic acid oligomers. In such a geometry for normal nucleic acid dinucleoside monophosphates, one would expect the base proton U° H-5 to be shifted upfield due to the shielding effect of adenine. However, what is observed is negligible downfield shift for U° H-5, contrary to this expectation. In addition the A^s H-2 displays significant high-field shifts which prima facie is perplexing.

A conformational analysis for A^{s}pU° similar to what was undertaken for U°pA^s is meaningless because the magnitude of the dimerization shift is so small that fitting the data in terms of the various conformers would be futile. Assuming a similar conformational blend for A^{s}pU° as for U°pA^s, the computed shieldings in the g^-g^-, g^+t, g^+g^+, and tg^+ conformers (Figure 6) are given in Tables VII and VIII (see paragraph at end of paper regarding supplementary material). It is remarkable to note that the U° H-5 of -pU° is little shielded in the g^-g^- of A^{s}pU° whereas the U° H-5 of U°p- in the g^-g^- of U°pA^s (Table V) is shielded to the extent of 0.37 ppm. In this g^-g^- geometry for A^{s}pU°, the base planes are separated by only 3–4 Å but the horizontal distance (ρ) between the centers of the rings is very large such that most of the protons of the uridine base have ρ values between 5 and 7 Å (Table IX, supplementary material) and hence little shielding or moderate deshielding. Even though the ω', ω angles in A^{s}pU° (ω = 260°, ω' = 280°) are very close to those for U°pA^s (ω' = 255°, ω = 270°), there are major differences in the gross morphology of the g^-g^- conformations of U°pA^s and A^{s}pU° (compare Figures 5 and 6). Further, the computed dimerization shift for A^s H-2 is totatly different from what is observed for A^{s}pU°. These observations make it unmistakably clear that in high anti systems the geometry is very much sequence dependent. This is the first time a significant difference in the spatial configuration of sequence isomers was observed and might have implications on their self-associative properties.

Table X: Variation of Chemical Shifts and Coupling Constants with Temperature for A^spU^o

temp (°C)	unit	chemical shift (Hz) 1′	2′	3′	4′	5′	5″	2	5
15	A^sp	893.9	490.0	426.0	296.0	154.2	110.2	1244.9	
	-pU^o	878.2	631.7	397.0	329.5	242.8	200.0		563.8
22	A^sp	896.4	496.9	438.8	299.0	159.7	118.0	1243.5	
	-pU^o	880.3	630.5	402.6	329.3	247.0	208.6		567.3
45	A^sp	930.9	517.8	435.1	312.5	137.8	101.6	1331.4	
	-pU^o	880.0	624.6	400.3	338.2	221.0	195.3		569.3
85	A^sp	938.0	527.6	446.9	319.7	140.5	106.7	1346.8	
	-pU^o	888.5	618.5	401.8	337.5	214.7	200.9		569.0

		coupling constants (Hz) $J_{1',2'}$	$J_{2',3'}$	$J_{3',4'}$	$J_{4',5'}$	$J_{4',5''}$	$J_{5',5''}$	$J_{3',P}$	$J_{4',P}$	$J_{5',P}$	$J_{5'',P}$	$J_{2',4'}$
15	A^sp	7.3	3.6	4.1	3.3	5.4	−12.7	7.2				
	pU^o	5.8	1.2	4.2	2.8	4.5	−11.8		1.1	5.3	5.7	
22	A^sp	6.7	3.4	5.1	3.2	5.2	−12.8	7.2				0.6
	pU^o	5.8	1.9	4.5	2.9	4.8	−11.8		1.5	4.8	5.7	0.3
45	A^sp	6.9	3.1	4.1	4.2	6.1	−12.5	7.2				0.5
	pU^o	5.4	0.8	3.0	3.6	5.4	−12.0		1.1	5.4	5.7	0.5
85	A^sp	6.8	2.7	3.8	4.4	6.3	−12.4	7.2				0.8
	pU^o	5.6	0.9	3.3	4.3	5.6	−12.0		0.6	5.8	6.1	0.5

Formation of Base-Paired Duplexes. The anomalous chemical shift data for A^spU^o has been recently rationalized on the basis of the formation of self-complementary base-paired duplexes (Mitra et al., 1980). In Figure 7 we have reproduced the structure of this duplex from Sarma (1980c). It may be noted that the duplex is stabilized by Watson–Crick hydrogen bonding and by strong interstrand adenine–adenine stacking interactions. It may also be noted that in Figure 7 in each strand there is little base–base overlap between A^s and U^o. In order to further verify the formation of miniature double helices, we have studied the ^1H NMR spectra of 20 mM solutions of A^spU^o as a function of temperature and have completely analyzed the spectra using computer simulation at 15, 22, 45, and 85 °C. The complete set of chemical shifts and coupling constants are given in Table X. The data show that with increasing temperature, all the protons of A^sp segment shift downfield, and at 85 °C they reach a value very close to that observed in the monomer A^sp. Further the temperature has only very little effect on the shift data of the -pU^o residue. These observations are in elegant agreement with our hypothesis (Mitra et al., 1980) that A^spU^o at high concentrations and low temperatures forms miniature double helices and elevation of temperature melt these double helices.

The coupling constant data in Table X indicate that with decreasing temperature, the only backbone torsion that gets affected significantly is C-4′–C-5′ (ψ). The magnitude of $J_{4',5'}$ and $J_{4',5''}$ decrease as the temperature is lowered; i.e., the sum of $J_{4',5'}$ and $J_{4',5''}$ for the -pU^o segment is 7.3 Hz at 15 °C and 9.9 Hz at 85 °C. This change of 2.7 Hz in the sum indicates that the population of *gg* decreases with increasing temperature. At low temperature the C-4′–C-5′ of the -pU^o segment prefers *gg* orientation. In other words the formation of a miniature double helix is accompanied by the increase in *gg* population for the backbone torsion (ψ). There are changes in other coupling constants, such as $J_{2',3'}$ and $J_{3',4'}$ which seem to increase with decrease in temperature and reflect a conformational adustment in the sugar geometry. The coupling constants $J_{5',P}$ and $J_{5'',P}$ also decrease with the formation of duplex; i.e., the population of *g′g′* orientation becomes more preferred.

In order to determine whether U^opA^s forms miniature duplexes like A^spU^o we have investigated the concentration dependence of the chemical shifts of the exchangeable amino protons in H_2O at 2 °C and that of the base protons in D_2O at 5 °C. The data are shown in Figure 8. Mitra et al. (1980) have reported that the base proton H-2 of adenine of A^spU^o is very sensitive to concentration; in fact the A^s H-2 moves upfield by as much as 150 Hz (270-MHz system) in the concentration range 5–50 mM (Mitra et al., 1980). Figure 8 shows that this is not the case for U^opA^s-; in fact the high-field shift is only about 20 Hz in the above range. The almost identical behavior for the shifts of H-2 of adenine in U^opA^s and the mononucleotide pA^s suggests that the source or the upfield shift with increasing concentration is most likely due to aggregation. This information along with the observation that the shift of U^o H-5 and A^s 6-NH_2 (Figure 8) are practically invariant with concentration clearly indicates that U^opA^s has no proclivity to form miniature double helices as its sequence isomer A^spU^o.

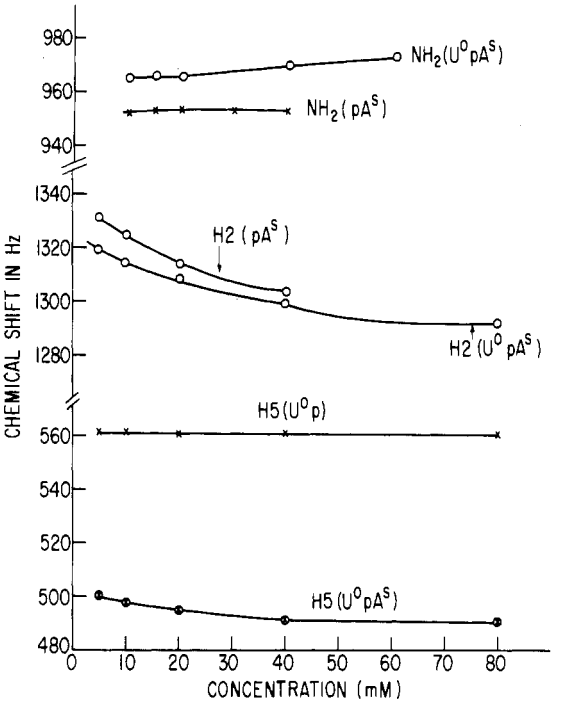

FIGURE 8: Concentration dependence of the hydrogen-bonding adenine NH_2 and the base protons of U^opA^s.

Spatial Configuration of High Anti Polynucleotides and Their Biological Relevance. From circular dichroism studies

where very dilute solutions ($\simeq$0.1 mM) are employed, it has been shown that $U^{o}pA^{s}$ assumes a left handed stacked conformation while $A^{s}pU^{o}$ does not assume a stacked conformation at all (Ikehara et al., 1980). These results are confirmed by the present NMR studies which also show that in the left handed stack of $U^{o}pA^{s}$, the pyrimidine part of A^{s} overlaps with the uracil of U^{o} (Figure 5) and that in $A^{s}pU^{o}$, there is little base–base overlap. In concentrated solutions (>10 mM $A^{s}pU^{o}$, but not $U^{o}pA^{s}$, forms a base-paired duplex which is stabilized by interstrand adenine–adenine stacking. $U^{o}pA^{s}$ exists in an equilibrium blend of mainly stacked conformation ($g^{-}g^{-}$) and skewed conformation ($g^{+}t$). The $g^{+}t$ conformation is one of the lowest energy conformations of $A^{s}pA^{s}$ according to the calculations of Fujii & Tomita (1976) and was recently found in a crystal structure of $I^{s}pA^{s}$ (Hamada et al., 1980).

The interstrand base–base stacking without intrastrand stacking observed in the $A^{s}pU^{o}$ duplex also occurs to a minor extent at the *pyrimidine*–purine sequence site of A-DNA and A-RNA (Arnott et al., 1969) and at the *purine–pyrimidine* sequence site of the vertical double helix (Olson, 1977). In these cases the helix is right handed. The experimentally determined torsion angles for $U^{o}pA^{s}$ and $A^{s}pU_{o}$ lie close to those projected by Sundaralingam & Yathindra (1977) rather than those of Olson (1977). For example, the experimental value for $g^{-}g^{-}$ for the cyclo dimers lie in the range ω' = 255–260°, ω = 270–280°; they are closer to that of Sundaralingam & Yathindra (1977) (ω' = 265°, ω = 275°) than to that of Olson (ω' = 268°, ω = 295°).

In order to determine the helical sense of the polynucleotide, we have mathematically polymerized the $g^{-}g^{-}$ conformations, and this generates a left handed single helix with the following parameters: rotation angle per residue (θ) −48.5°, height per residue (z) 3.4 Å; radius of helix (r) 6.4 Å, (S. Fujii, personal communication). This also means that the double helix for high anti nucleic acids containing repeating units of $A^{s}pU^{o}$ may also be left handed, as had been suggested by Sundaralingam & Yathrindra (1977).

One may indeed wonder what do high anti double helices have to do with biology. What is important to realize is that DNA and RNA are constructed by using flexible oligonucleotides which are conformationally pluralistic (Sarma, 1980b). This fact along with several lines of evidence suggests that nucleic acids are structures with considerable motional and dynamic characteristics—there is transient base-pair breakage and bubble formation, local fluctuations about the sugar–base torsion angle, and internal twisting and motions (Kallenbach et al., 1980; Sobell, 1980; Hurley et al., 1980; Rich et al., 1980; Olson, 1980). All these processes will endow the structure of DNA with considerable plasticity (Sarma et al., 1981), which in turn plays a crucial role in the control of gene expression. It is likely that a ligand or a protein may bind at one part of genomic DNA and cause local structural changes. The inherent plasticity of genomic DNA will enable propagation of these modulations at far away sites, cause structural distortions at these sites, and control the expression of genome The present study reveals that a simple distortion such as causing a change in χ to high anti values can cause the local structure to assume left handed helical configurations and thereby affect the expression of genomic information from that region.

Acknowledgments

We thank Dr. S. Fujii for calculation of helical parameters.

Supplementary Material Available

Tables VII–IX giving shielding and separation data for $A^{s}pU^{o}$ (3 pages). Ordering information is given on any current masthead page.

References

Arnott, S., & Hukins, D. W. L. (1972) *Biochem. Biophys. Res. Commun. 47*, 1504.
Arnott, S., Dover, S. D., & Wonacott, A. J. (1969) *Acta Crystallogr., Sect. B B25*, 2192.
Arnott, S., Chandrasekaran, R., Birdsall, D. C., Leslie, A. G. W., & Ratliff, R. L. (1980) *Nature (London) 283*, 743.
Cheng, D. M., & Sarma, R. H. (1977) *J. Am. Chem. Soc. 99*, 7333.
Dhingra, M. M., & Sarma, R. H. (1979) in *Sterodynamics of Molecular Systems* (Sarma, R. H., Ed.) p 3, Pergamon Press, New York.
Dhingra, M. M., Sarma, R. H., Giessner-Prettre, C., & Pullman, B. (1978a) *Biochemistry 17*, 5815.
Dhingra, M. M., Sarma, R. H., Uesugi, S., & Ikehara, M. (1978b) *J. Am. Chem. Soc. 100*, 4969.
Drew, H., Takano, T., Tanaka, S., Itakura, K., & Dickerson, R. E. (1980) *Nature (London) 286*, 567.
Evans, F. E., & Sarma, R. H. (1974) *J. Biol. Chem. 249*, 4754.
Evans, F. E., & Sarma, R. H. (1975) *J. Am. Chem. Soc. 97*, 3215.
Ezra, F. W., Lee, C. H., Kondo, N. S., Danyluk, S. S., & Sarma, R. H. (1977) *Biochemistry 16*, 1977.
Fujii, S., & Tomita, K. (1976) *Nucleic Acids Res. 3*, 1973.
Govil, G. (1976) *Biopolymers 15*, 2277.
Govil, G., & Saran, A. (1971) *J. Theor. Biol. 33*, 399.
Govil, G., Fisk, C., Howard, F. B., & Miles, H. T. (1977) *Nucleic Acids Res. 4*, 2573.
Hall, L. D., & Manville, J. F. (1968) *Carbohydr. Res. 8*, 295.
Hamada, K., Matsuo, Y., Miyamae, A., Fujii, S., & Tomita, K. (1980) *Nucleic Acids Res. Symp. Ser. No. 8*, 157.
Hurley, I., Robinson, B. H., Scholes, C. P., & Lerman, L. S. (1980) in *Nucleic Acid Geometry and Dynamics* (Sarma, R. H., Ed.) p 253, Pergamon Press, New York.
Ikehara, M., Uesugi, S., & Yasumoto, M. (1970) *J. Am. Chem. Soc. 92*, 4735.
Ikehara, M., Uesugi, S., & Yano, J. (1974) *J. Am. Chem. Soc. 96*, 4966.
Ikehara, M., Uesugi, S., & Shida, T. (1980) *Chem. Pharm. Bull. 28*, 189.
Kallenbach, N. R., Mandel, C., & Engalnder, S. W. (1980) in *Nucleic Acid Geometry and Dynamics* (Sarma, R. H., Ed.) p 233, Pergamon Press, New York.
Kashitani, Y., Fujii, S., & Tomita, K. (1976) *Biochem. Biophys. Res. Commun. 69*, 1028.
Kim, S. H., Berman, H. M., Seeman, N. C., & Newton, M. D. (1973) *Acta Crystallogr., Sect. B B29*, 703.
Lee, C. H., & Sarma, R. H. (1975) *J. Am. Chem. Soc. 97*, 1225.
Lee, C. H., & Sarma, R. H. (1976) *J. Am. Chem. Soc. 98*, 3541.
Lee, C. H., Evans, F. E., & Sarma, R. H. (1975) *J. Biol. Chem. 250*, 1290.
Lee, C. H., Ezra, F. S., Kondon, N. S., Sarma, R. H., & Danyluk, S. S. (1976) *Biochemistry 15*, 3627.
Mitra, C. K., Dhingra, M. M., & Sarma, R. H. (1980) *Biopolymers 19*, 1435.
Mitra, C. K., Sarma, M. H., & Sarma, R. H. (1981) *Biochemistry* (in press).
Olson, W. K. (1976) *Biopolymers 15*, 859.
Olson, W. K. (1977) *Proc. Natl. Acad. Sci. U.S.A. 74*, 1775.
Olson, W. K. (1980) in *Nucleic Acid Geometry and Dynamics* (Sarma, R. H., Ed.) p 388, Pergamon Press, New York.

Olson, W. K., & Dasika, R. D. (1976) *J. Am. Chem. Soc. 98*, 5371.
Pullman, B., & Saran, A. (1976) *Prog. Nucleic Acid Res. Mol. Biol. 18*, 215.
Pullman, B., Perahia, D., & Saran, A. (1972) *Biochem. Biophys. Res. Commun. 48*, 636.
Remin, M., & Shugar, D. (1972) *Biochem. Biophys. Res. Commun. 48*, 636.
Rich, A., Quigley, G. J., & Wang, A. H.-J. (1980) in *Nucleic Acid Geometry and Dynamics* (Sarma, R. H., Ed.) p 273, Pergamon Press, New York.
Rosenberg, J. M., Seeman, N. C., Day, R. O., & Rich, A. (1976) *J. Mol. Biol. 104*, 145.
Sarma, R. H. (1980a) in *Nucleic Acid Geometry and Dynamics* (Sarma, R. H., Ed.) p 1, Pergamon Press, New York.
Sarma, R. H. (1980b) in *Nucleic Acid Geometry and Dynamics* (Sarma, R. H., Ed.) p 143, Pergamon Press, New York.
Sarma, R. H. (1980c) in *Nucleic Acid Geometry and Dynamics* (Sarma, R. H., Ed.) p 83, Pergamon Press, New York.
Sarma, R. H., & Danyluk, S. S. (1977) *Int. J. Quantum Chem., Quantum Biol. Symp. 4*, 269.
Sarma, R. H., Mitra, C. K., & Sarma, M. H. (1981) in *Biomolecular Stereodynamics* (Sarma, R. H., Ed.) Vol. 1, Adenine Press, New York (in press).
Seeman, N. C., Rosenberg, J. M., Suddath, F. L., Kim, J. J., & Rich, A. (1976) *J. Mol. Biol. 104*, 109.
Sobell, H. M. (1980) in *Nucleic Acid Geometry and Dynamics* (Sarma, R. H., Ed.) p 289, Pergamon Press, New York.
Sundaralingam, M. (1973) *Jerusalem Symp. Quantum Chem. Biochem. 5*, 417.
Sundaralingam, M. (1975) *Structure and Conformation of Nucleic Acids and Protein–Nucleic Acid Interactions* (Sundaralingam, M., & Rao, S. T., Eds.) p 487, University Park Press, University Park, PA.
Sundaralingam, M., & Yathindra, N. (1977) *Int. J. Quantum Chem., Quantum Biol. Symp. 4*, 285.
Sundaralingam, M., & Westhof, E. (1979) *Int. J. Quantum Chem., Quantum Biol. Symp. 6*, 115.
Tomita, K., Yoneda, M., Fujiwara, T., & Ikehara, M. (1972) *Acta Crystallogr., Sect A A28*, 545.
Wang, A. H.-J, Quigley, G. J., Kolpak, F. J., Crawford, J. L., van Boom, J. H., van der Marel, G., & Rich, A. (1979) *Nature (London) 282*, 680.
Yathindra, N., & Sundaralingam, M. (1974) *Proc. Natl. Acad. Sci. U.S.A. 71*, 3325.
Yathindra, N., & Sundaralingam, M. (1976) *Nucleic Acids Res. 3*, 729.

A Heterologous Immunoglobulin Chain Recombinant Carries a Distinct Site for Dinitrophenyl and Obeys the Common Hapten Binding Mechanism†

Raphael Zidovetzki, Yoav Blatt, and Israel Pecht*

ABSTRACT: A heterologous recombinant of the immunoglobulin α heavy chain derived from MOPC-460 and the λ light chain from MOPC-315 was prepared. This $H^{460}L^{315}$ hybrid binds N^{ϵ}-(2,4-dinitrophenyl)-L-lysine (DNPL) with an affinity of 1.6×10^4 M^{-1} (7 °C). This Ig–hapten complex exhibits an absorption spectrum which is different from those observed for each of its parent–DNPL complexes. Very small quenching is caused in the intrinsic fluorescence of the hybrid upon hapten binding, as contrasted by the large quenching of the parent molecules. Chemical relaxation kinetic measurements show that $H^{460}L^{315}$ exists in solution in two conformations which exchange with a relaxation time of 20 ms (7 °C). This transition is accompanied by a change in the fluorescence quantum yield of the protein. DNPL binds to both conformers at comparable fast, though not diffusion-controlled, rates. The equilibrium between the two conformers is shifted upon hapten binding, and the two complexes exchange at a faster rate than the free protein conformers. Thus $H^{460}L^{315}$ carries a new binding site for DNPL but follows the common mechanism of hapten binding as that observed for other immunoglobulins. These properties of the hybrid should be closely related to the interactions between its constituting domains.

The heavy and light chains constituting immunoglobulins can be separated, after mild reduction, in dissociating solvents. Upon removal of these solvents, the separated chains can regain their native conformation and reassociate. When heavy and light chains from different parental molecules are reacted, new antibodies may be formed. Thus homologous or heterologous recombinant molecules can be prepared (Nisonoff et al., 1975; Dorrington & Tanford, 1968). Extensive studies of the recombination process revealed preferential homologous reassociations and the predominant role of the V[1] domains in that preference [cf., for example, de Preval & Fougereau (1976) and Bunting et al. (1977)]. Recent studies of the Ig gene structure (Schilling et al., 1980; Early et al., 1980) suggest that this preferential association is selected already at that level. The changes in the V_H–V_L contact residues would therefore affect both the affinity between these domains and their interactions with antigens.

The hapten binding properties of homologous recombinants remained unchanged while those of heterologous recombinants

† From the Department of Chemical Immunology, The Weizmann Institute of Science, Rehovot, 76100, Israel. *Received February 9, 1981.* This work was supported by The Fritz Thyssen Foundation.

[1] Abbreviations used: DNPL, N^{ϵ}-(2,4-dinitrophenyl)-L-lysine; H, heavy chain of immunoglobulin; $H^{460}L^{315}$, immunoglobulin recombinant composed of heavy chain from M-460 and light chain from M-315; Ig, immunoglobulin; L, light chain of immunoglobulin; L_{2cov}, light chain dimer from M-315 with disulfide bond between the chains; L_{2ncov}, light chain dimer from M-315 with reduced and alkylated disulfide bond; M-315, IgA secreted by MOPC-315 plasmacytoma; M-460, IgA secreted by MOPC-460 plasmacytoma; PBS, 0.01 M sodium phosphate buffer (pH 7.4)–0.15 M sodium chloride; V, variable region of immunoglobulin.

0006-2960/81/0420-5011$01.25/0